

분자 동역학을 이용한 점 결함 및 극 저 에너지 실리콘 이온 주입에 관한 연구

A Study on the Silicon Point Defects and Ultra-Low Energy Si Ion Implantation using Classical Molecular Dynamics

Jeong-Won Kang, Myung-Sik Son, Ki-Ryang Byun, and Ho-Jung Hwang

Semiconductor process & Device lab., Department of Electronic engineering, Chung-Ang Univ.

E-mail : kok@semilab3.ee.cau.ac.kr

Abstract

We have calculated ultra-low energy silicon-self ion implantations and silicon damages through classical molecular dynamics simulation using empirical potentials. We tested whether the recently developed Environment-Dependent Interatomic Potential(EDIP) was suitable for ultra low ion implantation simulation, and found that point defects formation energies were in good agreement with other theoretical calculations, but the calculated vacancy migration energy was overestimated. The number of isolated defects that are produced by collision cascades are only a few of the total number of defects, and most of the damages are concentrated into amorphous-like pockets.

I. Introduction

Ion implantation is nowadays a standard technology in integrated circuit device fabrication. As the device dimensions shrink, a reliable description of implant profile and production of damage is needed for technological development. For semiconductor devices, whose physical dimensions are of order of nanometer[1], ultra low energy ion implants and reduction of thermal processing are necessary, resulting in more prominent channeling effects in the as-implanted profiles and less post-implant diffusion(TED). Therefore, analysis of ultra low energy ion implants is very interesting, but unfortunately, the experimental possibilities for studying the processes occurring inside silicon substrate during irradiation are quite limited. During ion implantation, the displacement and mixing of identical atoms in an atomic collision cascade and defects such as vacancy, interstitial, and cluster arise. Much of the effort in semiconductor process modeling has focused on ion implantation and damage annealing because of the great industrial importance of

these processes.[2] Although collision cascades in silicon have been studied extensively during recent years[3-9], mechanisms causing the damages are still not very well understood.

Sometimes we can predict some areas which could not be determined experimentally using molecular dynamics simulation. In recent years, molecular dynamics simulation has been used for a far more realistic description of ion implantation.[9,10,11] Because interatomic forces lie at the very heart of almost all physical and chemical phenomena, we must choose appropriate methods for molecular dynamics simulation. Fully quantum mechanical *ab initio* molecular dynamics simulations using LDA-DFT(local density approximation - density functional theory) to calculate the interatomic forces have been carried out.[12,13,14] These methods generally provide the most reliable and accurate results; however, these approaches are generally only applicable for sub-electronvolt energies and for ground state atoms, so at present they cannot be used to model an entire atomic collision cascade. Empirical tight-binding molecular dynamics(ETBMD) has recently been emerging as a useful and powerful scheme for atomistic simulation study of structural, dynamics, and electronic properties of realistic materials.[15-18] Although ETB methods are much faster than *ab initio* methods, ETB methods cannot model an atomic collision cascades. Some (usually significant) quantum effects are neglected in simulations using empirical potentials, and these simulations are likely to be fast. Empirical potentials also may be manipulated to isolate a certain physical effect that is generally not available to the first principles approach. Therefore, for ion implant simulation, empirical potentials are suitable.

In this paper, we present some more detail on ion implantation mechanism using fully classical molecular

dynamics simulation. Our research involves ultra low energy silicon ion implantation, damage, and point defects(Sec. III) of silicon materials. In Sec. II, we explain total energy calculation and interatomic force calculation for classical molecular dynamics simulation, and we compare the results of Stillinger-Weber interatomic potential[19] with the results of Environment-Dependent Inteatomic Potential(EDIP)[20].

II. Total Energy Calculation and Interatomic Force for Classical Molecular Dynamics

We use classical MD method to simulate point defects properties and full collision cascades. The need to model of large numbers of material properties has led to the development of many-body potentials. The total potential energy U_{total} describing interaction among N identical particles can be resolved into one-body, two-body, three-body,...etc. Because of the importance of silicon technology, a great deal of effort has been expended in determining empirical model potentials for use in modelling Si. We have chosen the Stillinger-Weber interatomic potential[19] for these simulation because it predicts satisfactorily point defects properties in comparison with first-principles predictions[21] and is constructed to reproduce properties of solid, amorphous, and liquid Si. SW interatomic potential appears to be the most popular in literature. Also, the recently developed Environment-Dependent Interatomic Potential(EDIP) by M. Z. Bazant et al. is applied to calculate point defect properties in order to obtain more accurate and efficient potential. In these formulations, the total potential energy of the system is written as a sum over atomic sites in the form

$$U_{total} = \sum_{i,j} v_2(r_{ij}) + \sum_{i,j < k} v_3(\vec{r}_{ij}, \vec{r}_{ik}) \quad (1)$$

where, $v_2(r_{ij})$ and $v_3(\vec{r}_{ij}, \vec{r}_{ik})$ describe the pair-interaction energy and the three-body interaction energy, respectively. $v_2(r_{ij})$ is the radial function and $v_3(\vec{r}_{ij}, \vec{r}_{ik})$ is the radial and angle function. In the EDIP, $v_2(r_{ij})$ and $v_3(\vec{r}_{ij}, \vec{r}_{ik})$ are dependant on the local atomic environment through effective coordination number, $Z_i = \sum_j f(r_{ij})$, where $f(r_{ij})$ is a cutoff function that determines the contribution to an atom's coordination from each of its neighbors. Since pair-interaction energy produces forces on the

two atoms, $-\nabla_{r_i} v_2(r_{ij})$, and a change in the angle produces bond-angle force on the three atoms, three-body force F_3 on ith atom is summed together three-body radial force and bond-angle force,

$$F_3 = -\nabla_{r_i} v_3(\vec{r}_{ij}, \vec{r}_{ik}) - \nabla_{\cos\theta} v_3(\vec{r}_{ij}, \vec{r}_{ik}). \quad (2)$$

$$\text{where, } \cos\theta = \frac{\vec{r}_{ij} \cdot \vec{r}_{ik}}{|\vec{r}_{ij}| |\vec{r}_{ik}|}.$$

Total energy E_{total} is the sum of total potential U_{total} and kinetic energy K .

$$E_{total} = U_{total} + K = U_{total} + \sum_i \frac{p_i^2}{2m_i} \quad (3)$$

where, p_i and m_i are the momentum and the mass of atom, respectively.

For point defect, the calculations were performed in a 63-, 64-, or 65-atoms with a fixed volume. For ion implantation, silicon lattices of the target are 64,000 atoms in 108Å x 108Å sides and 108Å depth. At the start of simulation, the undamaged silicon target is heated to 300K by giving all atoms appropriate velocities and displacements from their lattice sites. Initial velocity distribution assumes maxwell velocity distribution in the solid. In simulations, periodic boundary conditions are applied to the sides of the target. The collision cascades are initiated by giving one silicon atom with an energy of 200eV, 500eV, 1keV, or 2keV to the target.

III. Results and Discussions

1. Point Defect Formation and Migration

Typical point defects that may be formed during the fabrication of devices are the vacancy, the interstitial, and possibly the V-I complex. In this section we will discuss defect formation energy, vacancy migration, and Frankel pair formation energy. To find the lowest energy configurations of neutral point defects, we fully relaxed 63, 64, or 65 silicon atoms. The initial positions of the relaxing atoms are changed by random, small distances in each direction 0.1-0.3Å prior to the relaxation, and Newton dynamics is used to find the relaxed atom position.

The formation energy $E_f(Si_{I,V})$ of this Si defect can be defined as

$$E_f(Si_{I,V}) = E(Si + I, V) - \frac{N_{Si,I,V}}{N_{Si}} E(Si) \quad (4)$$

where, I is interstitial and V is vacancy. $E(Si + I, V)$ term is the total energy including defects, $E(Si)$ term

is the bulk atom total energy, $N_{Si,T}$ is number of silicon atoms including defects, and N_S is number of the bulk silicon atoms.

Table I shows the formation energy for the structures of V, T-I, H-I as obtained from *ab initio*[22-25], ETB[26,27], SW, and EDIP. SW almost consists with DFT/LDA calculations, but EDIP is more accurate for the calculation of the point defects formation energies. Frankel pair defect formation energies show 4.76eV in SW, 6.78eV in EDIP, and 6.55eV in GSP-ETB[26].

We calculated the vacancy migration energy barrier along the exchange path. Vacancy directly exchanges sites with one of the first nearest neighbors. Potential energy barriers according to the vacancy exchange path appear in Fig 1. The unrelaxed energy barrier showed 0.94eV in SW, and this result is in good agreement with previous theoretical calculation using GSP(Goodwin, Skinner, and Pettifor) ETB method[26]. This energy barrier gives 0.32eV after full relaxation. In the EDIP, the relaxed energy barrier showed 2.31eV. According to our study, although EDIP gives the reasonable description of point defect formation energy, the vacancy migration energy barrier is too high to explain the self-diffusion phenomena.

Ion channeling occurred in $\langle 110 \rangle$ directions. Therefore the penetration energy barrier of $\langle 110 \rangle$ directions was calculated using SW. Unrelaxed penetration energy was 27eV, and relaxed penetration energy was 6.5eV. We concluded that the penetration energy barrier of $\langle 110 \rangle$ directions is a little higher than the Si self-diffusion energy, 4.8 ± 0.4eV[28], because neutral interstitial moves along H-T-H, $\langle 110 \rangle$ split-T- $\langle 110 \rangle$ split, or $\langle 110 \rangle$ split-H- $\langle 110 \rangle$ split paths. This barrier is in good agreement with ion stop energy, 5eV, in MC ion implantation simulation.

2. Ultra Low Energy Si Self Ion Implant and Damage Production

Ultra low energy Si self ion implantation are initiated by giving one silicon atom with an energy of 200eV, 500eV, 1keV, or 2keV and $\langle 100 \rangle$ direction at tilt 10° to the target. In Fig. 2, the potential energy variations in four different collision cascades by Si ion in crystalline silicon are shown as a function of time. Kinetic energy of ions is lost by repulsive potential at short distance interactions. The higher the implant energy is, the more collisions happen during the same time and the period of kinetic energy loss shorter. In the case of 200eV, most of ion kinetic energy is lost by repulsive potential energy

after 0.3ps. In the case of 2keV, the ions are passed through the base target after 3.5 ps. The higher the implant energy is, the deeper the ions go inside the surface[Fig. 3(a)], but silicon lattice mean displacements are not relevant to implant energy[Fig. 3(b)]. In the case of 200eV, one interstitial was produced and displaced 5.2 Å during 1ps. For most of the interstitials produced by ion implants, the mean displacement shows 3Å.

Fig. 4 shows angle distribution as a function of time along with the four different ion implant energies. For 1keV Si ion implantation, angle distributions with time are shown in Fig. 4(a). Perfect diamond structure has only 109.47° . But the diamond structure deviates as time increases. Angle distributions depending on ion implantation energy at 5ps are shown in Fig. 4(b). The higher the implant energy is, the more deviation increases.

Fig. 5 shows the evolution of damage production with time. When four 2keV Si ions are implanted into $\langle 100 \rangle$ directions simultaneously at tilt 10° , the damage profiles after 3ps, 4ps, and 5ps are shown in Fig. 5(a)(b)(c), respectively. An atom that moves more than the first nearest neighbors distance(2.35Å in silicon) is considered as an interstitial. The initial position of this atom is defined as a vacancy, unless the atom is in half a nearest neighbor distance of a vacancy. After 4ps, more damages are produced. The ion implants result in the production of amorphous pockets containing more displaced atoms than those predicted by other results[9-11], because we did not use lattice generation. Fig. 5(d) shows damage profile after 5ps, when four 1keV Si ions implant into $\langle 100 \rangle$ directions simultaneously at tilt 22° . However, damage profiles are similar to other results[9-11].

IV. Conclusion

We tested whether the recently developed Environment-Dependent Interatomic Potential(EDIP) was suitable for ultra low ion implantation simulation, and found that point defects formation energies were in good agreement with other theoretical calculations[22-27], but vacancy migration energy was overestimated. Therefore, we used SW interatomic potential for ion implantation simulations. We observed from the classical molecular dynamics simulation that the higher the implant energy is, the more collisions happen during the same time and the shorter the period of kinetic energy loss is, and the number of isolated defects that are produced are only a few of the total number of defects. Most of the damages are concentrated into amorphous-like pockets.

V. References

[1] "National Technology Roadmap for Semiconductors", SIA, (1994)
 [2] T. Diaz de la Rubia, S. Coffa, P. A. Stok, and C. S. Rafferty, "Defect and Diffusion in Silicon Processing", MRS vol.469, Pittsburgh, Pennsylvania (1997)
 [3] K. Nordlund, M. Ghaly, and R. S. Averback, J. Appl. Phys. 83 (3), 1238 (1998)
 [4] S. Tian, S.J. Morris, M. Morris, B. Obradovic and A.F. Tasch, IEDM 96, 713 (1996)
 [5] S. Moifatt, IEDM 97, 5 (1997)
 [6] A. Sultan, M. Craig, S. Banerjee, S. List, T. Grider, and V. McNeil, IEDM 97, 29, (1997)
 [7] M. Jaraiz, G. H. Gilmer, and J. M. Poate, and T. D. de la Rubia, Appl. Phys. Lett. 68 (3), 409 (1996)
 [8] M.G. Grimaldi, L. Caicagno, and P. Musumeci, N. Frangis, and J. V. Landuyt, J. Appl. Phys. 81 (11), 7181 (1997)
 [9] E. Chason et al., J. Appl. Phys. 81 (10), 6513 (1997)
 [10] P. J. Bedrossian, M. J. Caturla, and T. D. de las Rubia, Appl. Phys. Lett. 70 (2), 176 (1997)
 [11] T. D. de la Rubia, Nucl. Instr. and Meth. in Phys. Res. B 120 (1996)
 [12] R.Car and M. Parrinello, Phys. Rev. Lett. 55(22), p.2471 (1985)
 [13] J. Zhu, T. D. de la Rubia, L. H. Yang, C. Mailhot, and G.H. Gilmer, Phys. Rev. B 54, 4741 (1996)
 [14] W.C. Lee, S. G. Lee, and K. J. Chang, J. Phys.: Condens. Matter 10, 995 (1998)
 [15] L. Goodwin, A.J. Skinner, and D.G. Pettifor, Europhysics Letter 9 (7) p.701 (1989)
 [16] I. Kwon, et al., Phys. Rev. B 49, p.7242 (1994)
 [17] P.B. Rasband, P.Claney, and K. Sheterom, ECS Vol96-4, p.261, (1996)
 [18] A.K. McManh and J.E. Klepeis, Phys. Rev. B 56, p.12250(1997)
 [19] F.H.Stillinginger and T.A. Weber, Phys. Rev. B 31 (8) p.5262 (1985)
 [20] M. Z. Bazant, E. Kaxiras, J. F. Justo, Phys. Rev. B 56, 8542 (1997)
 [21] D. Maroulas and R. A. Brown, Phys. Rev. B 47, 15562(1993)
 [22] K.C. Pandey, Phys. Rev. Lett. 57, 2287 (1986)
 [23] Y. Bar Yair, and J.D. Joannopoulos, Phys. Rev. Lett. 52, 1129 (1984)
 [24] P.J. Kelly and R. Car, Phys. Rev. 45, 6543 (1992)
 [25] H. Seong and L.J. Lewis, Phys. Rev. B 53, 9791 (1996)
 [26] E. G. Song, E. Kim, and Y.H. Lee, Phys. Rev. B 48, 1486 (1993)
 [27] L. Colombo, M. Tang, T. Diaz de la Rubia, and F. Cargnoni, Physica Scripta, T66, 207 (1996)
 [28] G.H. Gilmer, T.D. de la Rubia, D.M. Stock, and M. Jaraiz, Nucl. Instr. and Meth. in Phys. Res. B 102 (1995)
 [29] P.E. Blochl, E. Sinargassi, R. Car, D. B. Laks, W. Andreoni, and S. T. Pantelides, Phys. Rev. Lett. 70, 2435 (1993)

	DFT/LDA	ETB	SW	EDIP
V	3.3-4.3 ⁴⁾	3.68 ⁶⁾	2.72	3.49
T-I	3.7-4.8 ⁴⁾	4.3 ⁶⁾	4.82	4.33
H-I	3.3-4.4 ⁴⁾	4.93 ⁶⁾	6.58	5.34
Frakel		6.55 ⁶⁾	4.76	6.78
V migration	0.3 ¹²⁾	0.31-0.7 ¹⁾	0.32/0.94)	2.31/5.23)

Table 1. Formation energies of various Si point defects(in eV) compared with other calculation. The values in parentheses are the unrelaxed energies. (V:vacancy, T-I: tetrahedral interstitial, H-I: hexagonal interstitial)



Fig. 1. Vacancy migration energy barrier curves along exchange path using SW:(---)unrelaxed, (---)relaxed)

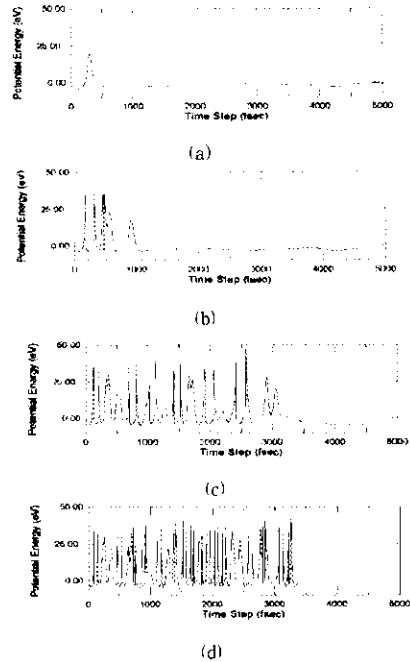


Fig. 2. Potential energy variations of implant ions as a function time. (a) 200eV, (b) 500eV, (c) 1000eV, and (d) 2000eV.

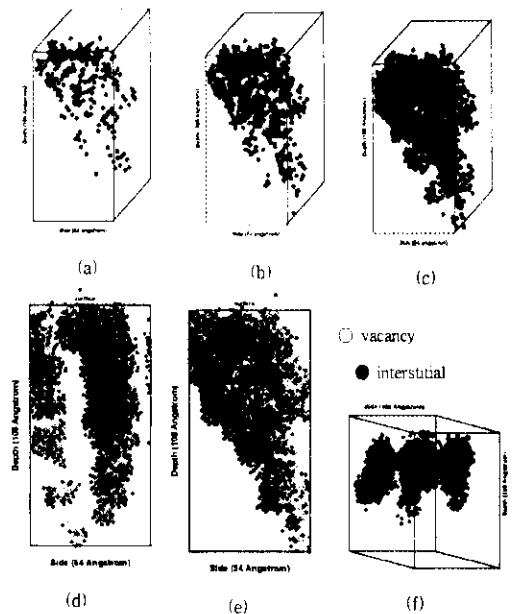


Fig. 5. The evolutions of damages production with time. When four 2keV Si ions are implanted into <100> directions simultaneously at tilt 10°, (a), (b), and (c) are shown damages profiles after 3ps, 4ps, and 5ps, respectively, and (d) and (e) are side views after 5ps. (f) is shown damages profiles after 5ps, when four 1keV Si ions are implanted into <100> directions simultaneously at tilt 10°